

**Conducting polymer functionalized single-walled carbon nanotube based chemiresistive biosensor for the detection of human cardiac myoglobin**

Nidhi Puri, Asad Niazi, Ashok M. Biradar, Ashok Mulchandani, and Rajesh

Citation: *Applied Physics Letters* **105**, 153701 (2014); doi: 10.1063/1.4897972

View online: <http://dx.doi.org/10.1063/1.4897972>

View Table of Contents: <http://scitation.aip.org/content/aip/journal/apl/105/15?ver=pdfcov>

Published by the *AIP Publishing*

---

**Articles you may be interested in**

[Single-walled carbon nanotubes based chemiresistive genosensor for label-free detection of human rheumatic heart disease](#)

*Appl. Phys. Lett.* **105**, 213701 (2014); 10.1063/1.4902447

[Self-formation of highly aligned metallic, semiconducting and single chiral single-walled carbon nanotubes assemblies via a crystal template method](#)

*Appl. Phys. Lett.* **105**, 093102 (2014); 10.1063/1.4895103

[Label-free detection of cardiac troponin-I using gold nanoparticles functionalized single-walled carbon nanotubes based chemiresistive biosensor](#)

*Appl. Phys. Lett.* **103**, 203703 (2013); 10.1063/1.4830223

[Unaltered electrical conductance in single-walled carbon nanotubes functionalized with divalent adducts](#)

*Appl. Phys. Lett.* **101**, 053116 (2012); 10.1063/1.4739495

[Piezoresistive pressure sensors with parallel integration of individual single-walled carbon nanotubes](#)

*J. Appl. Phys.* **109**, 064310 (2011); 10.1063/1.3555619

---

You don't still use this cell phone

or this computer

**Why are you still using an AFM designed in the 80's?**

**It is time to upgrade your AFM**

Minimum \$20,000 trade-in discount for purchases before August 31st

**Asylum Research is today's technology leader in AFM**

dropmyoldAFM@oxinst.com

**OXFORD INSTRUMENTS**  
The Business of Science®



## Conducting polymer functionalized single-walled carbon nanotube based chemiresistive biosensor for the detection of human cardiac myoglobin

Nidhi Puri,<sup>1,2</sup> Asad Niazi,<sup>2</sup> Ashok M. Biradar,<sup>1</sup> Ashok Mulchandani,<sup>3,a)</sup> and Rajesh<sup>1,a)</sup>

<sup>1</sup>CSIR-National Physical Laboratory, Dr. K. S. Krishnan Road, New Delhi 110012, India

<sup>2</sup>Department of Physics, Faculty of Natural Sciences, Jamia Millia Islamia, New Delhi 110025, India

<sup>3</sup>Department of Chemical and Environmental Engineering, University of California, Riverside, California 92521, USA

(Received 4 August 2014; accepted 28 September 2014; published online 14 October 2014)

We report the fabrication of a single-walled carbon nanotube (SWNT) based ultrasensitive label-free chemiresistive biosensor for the detection of human cardiac biomarker, myoglobin (Ag-cMb). Poly(pyrrole-co-pyrrolepropylic acid) with pendant carboxyl groups was electrochemically deposited on electrophoretically aligned SWNT channel, as a conducting linker, for biomolecular immobilization of highly specific cardiac myoglobin antibody. The device was characterized by scanning electron microscopy, source-drain current-voltage ( $I$ - $V$ ), and charge-transfer characteristic studies. The device exhibited a linear response with a change in conductance in SWNT channel towards the target, Ag-cMb, over the concentration range of 1.0 to 1000 ng ml<sup>-1</sup> with a sensitivity of ~118% per decade with high specificity. © 2014 AIP Publishing LLC.

[<http://dx.doi.org/10.1063/1.4897972>]

Cardiac myoglobin (cMb), a monomeric hemeprotein, is an important biological index for the diagnosis of acute myocardial infarction (AMI). Though cMb is not highly cardiac specific due to its abundant presence in myocardial as well as skeletal muscle cells, its small size with molecular dimension of 3 nm × 4 nm × 5 nm and molar volume of 1.87 × 10<sup>4</sup> cm<sup>3</sup> mol<sup>-1</sup> quickly releases it into blood circulation within 1 to 3 h after symptom onset and reaches a maximum between 6 and 12 h, subsequently returning to the baseline within 24–48 h.<sup>1,2</sup> In the first 1 h of onset of myocardial infarction, the cMb level shoots up to 200 ng ml<sup>-1</sup> from the normal level of 30 to 90 ng ml<sup>-1</sup> in human blood and can reach as high as 900 ng ml<sup>-1</sup> during the peak hour.<sup>3</sup> This high predictive value together with a high sensitivity makes it a valuable biomarker for the early screening test of AMI.

Recent advancement in biological sensing techniques has transformed the conventional detection techniques such as piezoelectric,<sup>4</sup> optical,<sup>5</sup> and electrochemical<sup>6</sup> to simpler and miniaturized methods, which are comparatively much more sensitive, reliable, and stable. One dimensional nanomaterials such as nanotubes, nanowires, and nanorods are being increasingly used in the miniaturized biosensing research field because of their sensitivity to electronic perturbation, which allows high sensitivity and rapid analyte detection.<sup>7–10</sup> Among these materials, semiconducting single walled carbon nanotubes (SWNTs), hollow cylinders of sp<sup>2</sup> bonded carbon atoms with diameter of 1–2 nm have emerged as an efficient transducer<sup>11–13</sup> for making chemiresistor/field effect transistor (FET) devices because of their good electrical conductivity due to large carrier mobility.<sup>14–16</sup> SWNTs have few defects, are chemically stable and inert, and their large surface to volume ratio makes them sensitive to any surface adsorption of biomolecules, with large, easily measurable changes in FET device resistance/conductance.<sup>17,18</sup>

However, the proper immobilization of biomolecules to the matrix of these one dimensional SWNT devices remains of concern. Biomolecules such as peptides, proteins, and antibodies possess special affinity to their complementary species and hence an efficient surface immobilization technique is required to be established to enhance the immobilization amount and ultimate detection capacity. The biomolecular immobilization may either be carried out by a physical or a covalent linkage technique. However, physical immobilization is prone to weak bonding, and covalent linkage, though strong, requires a linker molecule, which affects the electrical connectivity of SWNT to the biomolecule.

Conducting polymers have been used as the most promising biomolecular immobilizing matrices because of their extraordinary electrochemical properties arising from their conjugated  $\pi$ -electron backbone.<sup>19–21</sup> Hence, we have used a functionalized conducting copolymer poly(pyrrole-co-pyrrolepropylic acid) (PPy-PPa) composed of two contrasting monomers: highly conducting pyrrole (Py) and low conducting pyrrolepropylic acid (Pa), as an organic conjugate linker for biomolecular covalent immobilization of SWNT. The PPy-PPa copolymer film shows good electrical conductivity, while maintaining the semiconductor function of the device and its feasibility in one dimensional carbon nanomaterial based FET device has been investigated via source-drain current vs voltage ( $I$ - $V$ ) measurements and FET characteristics. While there are previous studies on the one dimensional carbon nanomaterial based chemiresistive biosensors, in this work, we have utilized the polymer composites in such devices to provide efficient biomolecular immobilization for the quantitative detection of cardiac biomarkers.

In this paper, we describe the fabrication of a chemiresistive biosensor for the detection of human cardiac biomarker, myoglobin protein antigen (Ag-cMb) by electrochemical deposition of conducting copolymer PPy-PPa on  $p$ -type SWNT electrophoretically aligned between gold microelectrodes.

<sup>a)</sup>Electronic addresses: rajesh\_csir@yahoo.com and adani@enr.ucr.edu

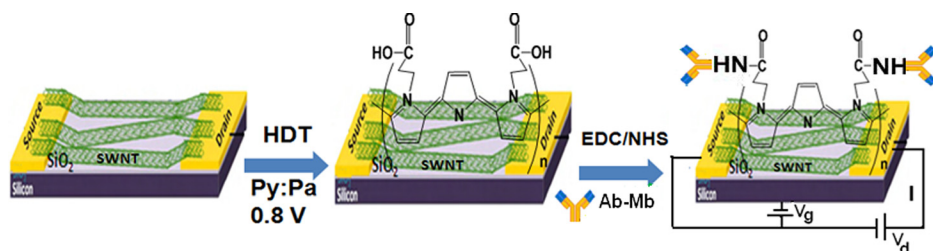


FIG. 1. Schematic representation of the stepwise fabrication process of Ab-Mb/PPy-PPa/SWNT device.

The highly specific cardiac myoglobin protein antibody, Ab-Mb, was covalently immobilized through its amino group to the pendant carboxyl group of the electrodeposited copolymer PPy-PPa film by a carbodiimide coupling reaction. The fabrication process of the device is schematically represented in Figure 1. Scanning electron microscopy (SEM), energy dispersive X-ray analysis (EDAX),  $I$ - $V$  measurements, and FET characteristics were used to characterize the device formation, its performance and sensing mechanism.

Monoclonal mouse anti-human cardiac myoglobin (Ab-Mb; Cat 4M23), Myoglobin derived from human heart tissue (Ag-cMb; Cat 8M50), and C-reactive protein (Ag-CRP; Cat 8C72) were procured from Hytest (Turku, Finland). Mouse immunoglobulin-G (Ag-IgG; Cat IGP3) was obtained from GENEI, Bangalore. Pyrrole, pyrrolepropyic acid, sodium *p*-Toluene sulphonic acid (*p*-TSA), *N*-(3-dimethylamino-propyl)-*N'*-ethyl carbodiimide hydrochloride (EDC), *N*-hydroxy succinimide 98% (NHS) were obtained from Sigma-Aldrich chemicals. 1-hexadecanethiol (HDT) was purchased from Merck Schuchardt. The SWNTs (SWNT-COOH, 80%–90% purity; bundle diameter: 4–5 nm) were purchased from Carbon Solution, Inc. (Riverside, CA, USA). All other chemicals/reagents were of analytical grade and used without further purification.

A suspension of SWNT in *N,N*-dimethylformamide (DMF) ( $0.01 \text{ mg ml}^{-1}$ ) was prepared by centrifugation at  $31000 \times g$  for 90 min.  $2.0 \mu\text{l}$  of the above dispersed SWNT suspension were aligned across a pair of  $3 \mu\text{m}$  apart micro-fabricated gold electrodes using A.C. dielectrophoresis at 5 MHz frequency with a peak-to-peak amplitude of 1.5 V, followed by annealing at  $300^\circ\text{C}$  for 1 h under a reducing environment ( $\text{N}_2$  with 5%  $\text{H}_2$ ).<sup>17</sup> A mixture of ethanolic solution of 0.25 mM 1-hexadecanethiol (HDT) and water (1:1 v/v) was drop cast over the SWNT aligned gold microelectrodes for 15 min to deposit a self assembled monolayer (SAM) of HDT on the exposed gold surface. Such a SAM of HDT on gold surface has been reported earlier to produce an electro-inactive gold surface for electrochemical reactions.<sup>22</sup> Thus, SAM of HDT prevents the undesired electrochemical deposition of conducting copolymer on the exposed gold surface during electro-polymerization, allowing electro-deposition only on the aligned SWNT channel. For electrochemical polymerization, the SWNT/Au-HDT microelectrode was taken as a working electrode with Ag/AgCl wire as a reference electrode and platinum needle as a counter electrode using PGSTAT302N, AUTOLAB instrument from Eco Chemie, connected to a probe station, Micromanipulator model 450PM-B for electrical contact to the source and drain electrodes (Fig. 2). The PPy-PPa with a controlled film thickness was electrochemically deposited on SWNT/Au-HDT from a degassed aqueous solution containing 0.1 M pyrrole (Py),

0.03 M pyrrolepropyic acid (Pa), and 0.1 M *p*-TSA, at a fixed bias voltage of 0.8 V vs Ag/AgCl by controlling the passage of current. The pendant carboxyl groups of the PPy-PPa deposited on SWNT were activated by drop casting an aqueous solution containing 0.03 M NHS and 0.15 M EDC for 1 h followed by washing with distilled water and dried under  $\text{N}_2$  gas flow. The activated PPy-PPa/SWNT was incubated with phosphate buffer saline (PBS; pH 7.4) containing  $100 \mu\text{g ml}^{-1}$  Ab-Mb, for 3 h at  $4^\circ\text{C}$ , for biomolecular immobilization, followed by washing with PBS (pH 7.4) and dried under  $\text{N}_2$  gas flow to obtain the desired Ab-Mb/PPy-PPa/SWNT nanodevice. The device was passivated with 0.1% bovine serum albumin (BSA) in PBS to block the nonspecific binding sites of the SWNT channel as well as the unbound activated carboxyl group in PPy-PPa/SWNT, leaving only the active sites of specific Ab-Mb for immunoreaction interaction with complementary target antigen, Ag-cMb.

The device characterization and response measurement towards target Ag-cMb were carried out by monitoring the ( $I$ - $V$ ) characteristics in a range from  $-0.5 \text{ V}$  to  $+0.5 \text{ V}$ . These electrical characteristics of the device were monitored after each step of device fabrication and the resistance was calculated by taking the inverse of the slope of  $I$ - $V$  curve from  $-0.5$  to  $+0.5 \text{ V}$  (Fig. 3(a)). A decrease in source-drain current ( $I_{sd}$ ) of the SWNT device was observed upon SAM formation of HDT on the gold microelectrodes, which further decreased on electrodeposition of PPy-PPa film on SWNT, which may be attributed to a decrease in hole density at the interface upon transfer of electrons from the conjugated polymer to *p*-type SWNT. This has been substantiated by carrying out the FET characteristics studies of PPy-PPa/SWNT device (Fig. 3(b)) on both before and after electrodeposition of PPy-PPa on SWNT with a back gate voltage,  $V_g$ ,

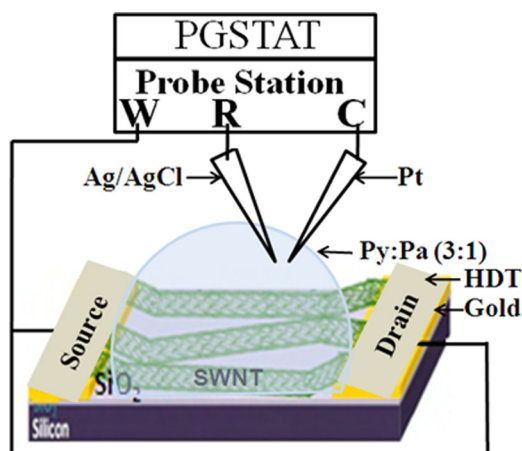


FIG. 2. Schematic representation of the electrochemical setup for the electrochemical deposition of PPy-PPa copolymer on SWNT device.



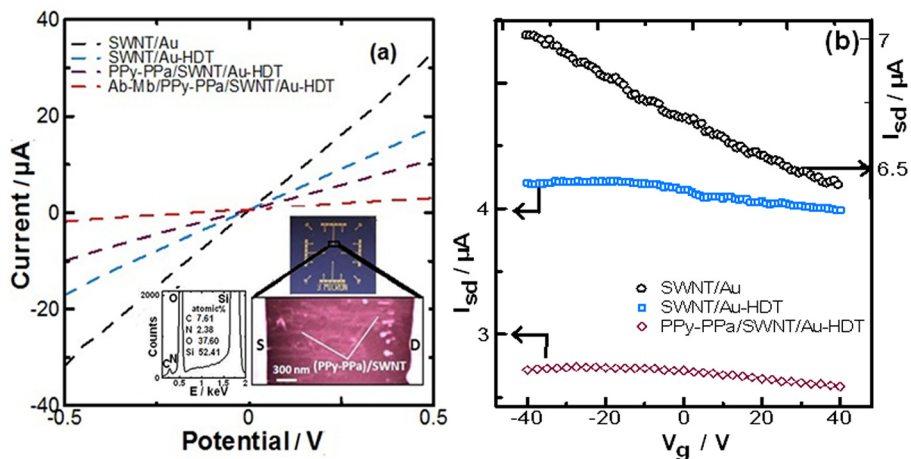


FIG. 3. (a) Current-Voltage ( $I$ - $V$ ) characteristics curves of the device at various stages of fabrication; Inset shows the micro-chip structure with a SEM image of PPy-PPa/SWNT/Au-HDT at 60.00 KX magnification; and EDAX scanning results for corresponding electrode; (b) FET characteristics curves for the corresponding PPy-PPa/SWNT/Au-HDT device.

in the range of  $-40$  to  $+40$  V, at a bias drain voltage ( $V_d$ ) of  $0.1$  V recorded on a Keithley semiconductor characterization system 2420. The charge/hole density ( $\rho$ ) in the PPy-PPa/SWNT-FET device was calculated by  $\rho = C\Delta V_T/eL$  (where  $C$  is the approximate capacitance,  $\Delta V_T$  = shift in threshold voltage,  $L$  = channel length) and the charge mobility of the holes,  $\mu = L^2 (dI_{sd}/dV_g)/CV_d$  (where  $V_d$  = drain voltage).<sup>17</sup> Figure 3(b) shows a typical  $p$ -type semiconducting behavior for pristine SWNT due to electron transfer from adsorbed oxygen,<sup>23</sup> with a charge mobility of  $1.03 \times 10^2 \text{ cm}^2 \text{ V}^{-1} \text{ S}^{-1}$ . A decrease in current was observed at a given voltage for the HDT treated SWNT device with a much lower charge mobility of  $0.39 \times 10^2 \text{ cm}^2 \text{ V}^{-1} \text{ S}^{-1}$  and a decrease in hole density of  $1.93 \times 10^7 \text{ cm}^{-1}$  with respect to pristine SWNT. This change in electrical phenomenon has been found to be contrary to earlier report, where an increased current was observed for SWNT FET after 8 h exposure treatment of the gold surface with HDT.<sup>24</sup> This may be understood on the basis of the surface coverage of the gold surface with HDT depending on treatment time. In our case, an exposure to HDT in aqueous ethanolic solution of critical ratio<sup>22</sup> with a small treatment time of 15 min perhaps did not give enough time for the thiols to diffuse into the SWNT-gold interface. This might have shifted away the Au Fermi level from the valence band of SWNT, modulating the local work function and thereby increases the charge injection barrier imparting a contact resistance (Schottky barrier). Further, it is interesting to note that after electrodeposition of the PPy-PPa film on SWNT/Au-HDT, even though the  $I_{sd}$  decreased significantly with a substantial decrease in hole density ( $1.28 \times 10^7 \text{ cm}^{-1}$  w.r.t. SWNT/Au-HDT), decrease in charge mobility ( $0.23 \times 10^2 \text{ cm}^2 \text{ V}^{-1} \text{ S}^{-1}$ ) was not as much, indicating a possible electrostatic gating effect due to electron charge transfer and scattering of charge carriers at the PPy-PPa/SWNT interface. The electrodeposition of PPy-PPa on SWNT was also characterized by SEM and EDAX analysis (the inset of Fig. 3(a)) with a LEO 440 PC; UK based digital scanning electron microscope. The SEM image shows well aligned PPy-PPa/SWNT, whereas the presence of nitrogen in the elemental analysis of EDAX spectra revealed the electrodeposition of PPy-PPa film on SWNT. Further, subsequent decrease in  $I_{sd}$  was observed in  $I$ - $V$  curve, upon covalent biomolecular immobilization of the PPy-PPa/SWNT with

Ab-Mb, and on its passivation with BSA due to the donation of electrons to SWNT from the electron rich basic amino acids such as arginine, histidine, and lysine of the protein backbone structure.<sup>25</sup>

The current/resistance behavior of the Ab-Mb/PPy-PPa/SWNT device was investigated towards the target protein antigen, Ag-cMb, in PBS (pH 7.4). Since no large appreciable increase in current was observed in PPy-PPa/SWNT at applied gate voltage from  $0$  to  $-30$  V, sensing performance of the device was carried out as a chemiresistive biosensor, without a gate voltage. The device was incubated with a  $2.0 \mu\text{l}$  sample volume of different concentrations of Ag-cMb in PBS ranging from  $0.1$  to  $1000 \text{ ng ml}^{-1}$ , for a period of 1 min, followed by washing with distilled water and dry under  $\text{N}_2$  gas flow.  $I$ - $V$  measurements were taken under dry condition. It was found that the device on incubation with each increasing concentration of Ag-cMb exhibited a decreasing trend of current conductance in SWNT with antigen-antibody complex formation on immunoreaction at PPy-PPa/SWNT surface. We attribute this to electron charge transfer to SWNT from the adsorbed biomolecules on immunoreaction. Figure 4 shows the normalized calibration curve ( $\Delta R/R_0 = [(R)_{\text{after immunoreaction}} - R_0]/R_0$ ) for Ab-Mb/PPy-PPa/SWNT device in a concentration

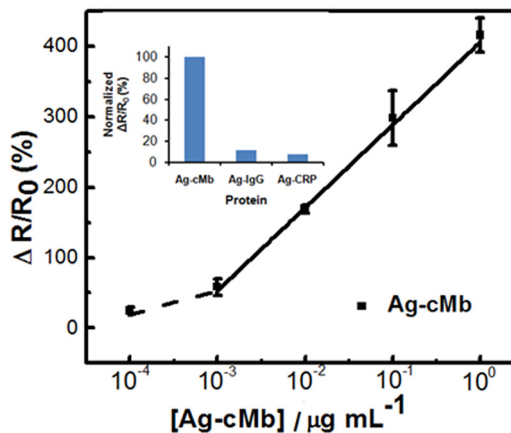


FIG. 4. Concentration dependence calibration curve of Ab-Mb/PPy-PPa/SWNT device for  $[\text{Ag-cMb}]$ . Each data point is an average of the measurements from three individual devices and error bars represent  $\pm 1$  standard deviation; Inset: normalized  $\Delta R/R_0$  (%) response of the device for  $[\text{Ag-IgG}]$  and  $[\text{Ag-CRP}]$  with respect to  $[\text{Ag-cMb}]$ .

range of 0.1 to 1000 ng ml<sup>-1</sup> of Ag-cMb in PBS, where R<sub>0</sub> and R are the device resistance measured before and after exposure to Ag-cMb, respectively. The device exhibited a linear response in  $\Delta R/R_0$  over a concentration range of 1 to 1000 ng ml<sup>-1</sup> Ag-cMb with a sensitivity of  $\sim 118\%$  per decade. This high sensitivity may be attributed to high Ab-Mb probe loading of PPy-PPa copolymer due to its active binding sites of pendant carboxylic groups and porous microstructure,<sup>26</sup> resulting in increased electron transfer to the SWNT on immunoreaction. The lowest detection limit of the device was estimated to 24.2 pg ml<sup>-1</sup> based on three times of signal-to-noise ratio ( $3\sigma/m$ ; where  $\sigma$  is standard deviation of the intercept and  $m$  is the slope of the linear curve), indicating to a much lower level detection of Ag-cMb than previously reported sensors.<sup>27,28</sup>

The specificity of the Ab-Mb/PPy-PPa/SWNT device was also investigated by monitoring its response to a non-specific protein, mouse Ag-IgG, and another cardiac specific biomarker, C-reactive protein (Ag-CRP), under identical conditions, as described for the specific target Ag-cMb. The inset of Figure 4 summarizes the normalized  $\Delta R/R_0$  (%) of the device on exposure to individual 100 ng ml<sup>-1</sup> Ag-IgG and Ag-CRP with respect to Ag-cMb. The device showed normalized response ( $\Delta R/R_0$ ) of 11.6% and 7.2% for Ag-IgG and Ag-CRP, respectively, with respect to Ag-cMb. These significantly smaller responses in resistance towards non-specific proteins due to non-occurrence of immunoreaction on the Ab-Mb/PPy-PPa/SWNT surface, indicating good selectivity of the device towards the specific target Ag-cMb.

In conclusion, we demonstrated a conducting copolymer functionalized SWNT based chemiresistive biosensor for the ultrasensitive detection of human cardiac biomarker myoglobin, cMb. PPy-PPa was electrochemically deposited on conducting SWNT channel, as a conducting linker, by making the gold electrodes (source-drain) surface electro-inactive in the working zone with a low defect density monolayer of 1-hexadecanethiol (HDT). The synergistic combination of Py and Pa monomers in PPy-PPa copolymer linker provided a covalent binding ability for efficient biomolecular immobilization with good biocompatibility. The charge transfer characteristic of the PPy-PPa/SWNT device showed electrostatic gating effect with large electron doping on SWNT. High protein Ab-Mb loading with strong covalent binding to PPy-PPa/SWNT, responsible for an increased immunoreaction with the target Ag-cMb, resulted in to a high sensitivity of  $\sim 118\%$  per decade Ag-cMb concentration. The high sensitivity, selectivity, and good biocompatibility of the device can provide a platform for the label free detection of the

target molecules, after appropriate optimization with real blood/serum, for clinical diagnosis in future.

We are grateful to Professor R. C. Budhani, Director, National Physical Laboratory, New Delhi, India, for providing research facilities. One of the authors, Nidhi Puri is thankful to CSIR for providing Senior Research Fellowship. A.M. is grateful for support from the W. Ruel Johnson Chair in Environmental Engineering.

- <sup>1</sup>J. C. Kendrew, G. Bodo, H. M. Dintzis, R. G. Parrish, H. Wyckoff, and D. C. Phillips, *Nature* **181**, 662 (1958).
- <sup>2</sup>G. Gros, B. A. Wittenberg, and T. Jue, *J. Exp. Biol.* **213**, 2713 (2010).
- <sup>3</sup>T. Olsson, K. Bergstrom, and A. Tore, *Clin. Chim. Acta* **138**, 31 (1984).
- <sup>4</sup>A. Janshoff, H. J. Galla, and C. Steinem, *Angew. Chem. Int. Ed.* **39**, 4004 (2000).
- <sup>5</sup>M. A. Cooper, *Nat. Rev. Drug Discovery* **1**, 515 (2002).
- <sup>6</sup>J. Wang, *Anal. Chim. Acta* **469**, 63 (2002).
- <sup>7</sup>Z. M. Liu, Y. Yang, H. Wang, Y. L. Liu, G. L. Shen, and R. Q. Yu, *Sens. Actuators, B* **106**, 394 (2005).
- <sup>8</sup>B. He, T. J. Morrow, and C. D. Keating, *Curr. Opin. Chem. Biol.* **12**, 522 (2008).
- <sup>9</sup>F. Patolsky, G. F. Zheng, and C. M. Lieber, *Anal. Chem.* **78**, 4260 (2006).
- <sup>10</sup>M. Trojanowicz, *TrAC-Trend Anal. Chem.* **25**, 480 (2006).
- <sup>11</sup>K. S. Vasu, K. Naresh, R. S. Bagul, N. Jayaraman, and A. K. Sood, *Appl. Phys. Lett.* **101**, 053701 (2012).
- <sup>12</sup>Rajesh, V. Sharma, N. K. Puri, R. K. Singh, A. M. Biradar, and A. Mulchandani, *Appl. Phys. Lett.* **103**, 203703 (2013).
- <sup>13</sup>C. B. Jacobs, M. J. Peairs, and B. J. Venton, *Anal. Chim. Acta* **662**, 105 (2010).
- <sup>14</sup>R. J. Chen, S. Bangsaruntip, K. A. Drouvalakis, N. W. S. Kam, M. Shim, Y. Li, W. Kim, P. J. Utz, and H. Dai, *Proc. Natl. Acad. Sci. USA* **100**, 4984 (2003).
- <sup>15</sup>J. Wang, *Electroanalysis* **17**, 7 (2005).
- <sup>16</sup>L. N. Cella, W. Chen, N. V. Myung, and A. Mulchandani, *J. Am. Chem. Soc.* **132**, 5024 (2010).
- <sup>17</sup>Rajesh, B. K. Das, S. Srinives, and A. Mulchandani, *Appl. Phys. Lett.* **98**, 013701 (2011).
- <sup>18</sup>J. Oh, G. Yoo, Y. W. Chang, H. J. Kim, J. Jose, E. Kim, J.-C. Pyun, and K.-H. Yoo, *Biosens. Bioelectron.* **50**, 345 (2013).
- <sup>19</sup>N. K. Guimard, N. Gomez, and C. E. Schmidt, *Prog. Polym. Sci.* **32**, 876 (2007).
- <sup>20</sup>T. Ahuja, I. A. Mir, D. Kumar, and Rajesh, *Biomaterials* **28**, 791 (2007).
- <sup>21</sup>Rajesh, N. Puri, S. K. Mishra, M. J. Laskar, and A. K. Srivastava, *Appl. Biochem. Biotechnol.* **172**, 1055 (2014).
- <sup>22</sup>S. Menolasina, *Ciencia* **11**, 87 (2003).
- <sup>23</sup>A. Star, J. C. Gabriel, K. Bradley, and G. Gruner, *Nano Lett.* **3**, 459 (2003).
- <sup>24</sup>X. Cui, M. Freitag, R. Martel, L. Brus, and P. Avouris, *Nano Lett.* **3**, 783 (2003).
- <sup>25</sup>K. Bradley, M. Briman, A. Star, and G. Gruner, *Nano Lett.* **4**, 253 (2004).
- <sup>26</sup>N. Puri, A. Niazi, A. K. Srivastava, and Rajesh, *Electrochim. Acta* **123**, 211 (2014).
- <sup>27</sup>S. Pakapongpan, R. Palangsantikul, and W. Surareungchai, *Electrochim. Acta* **56**, 6831 (2011).
- <sup>28</sup>S. S. Mandal, K. K. Narayan, and A. J. Bhattacharyya, *J. Mater. Chem. B* **1**, 3051 (2013).